Photon path-length distributions for transmission through optically turbid slabs

A. H. Gandjbakhche, G. H. Weiss, R. F. Bonner, and R. Nossal
National Institutes of Health, Bethesda, Maryland 20892
(Received 25 March 1993)

A discrete stochastic model is used to derive analytic expressions for various quantities relating to photon transport through an optically turbid slab. Several theoretical predictions, including those of the distributions of total path length, diffuse surface reemissions, and time-resolved point intensities, are examined by comparison with Monte Carlo simulations of a continuous-random-walk model of photon migration through a semi-infinite medium of finite thickness.

PACS number(s): 05.40.+j, 42.25.Fx

I. INTRODUCTION

In recent years considerable effort has been expended to develop optical techniques for medical diagnosis or therapy. Indeed, laser sources now are widely employed as surgical tools for excising, disrupting, or coagulating tissue [1,2]. Other widely investigated applications include photodynamic cancer therapy [3,4], measurement of microcirculatory blood flow [5], and blood pulse oximetry [6]. Lately much attention also has been given to devising methods for tomographic imaging of tissues, whereby nonionizing visible or near-visible radiation might be used to detect tumors [7,8] or to monitor physiological status such as regional blood oxygenation [9,10].

In order to effectively apply such techniques it is desirable to develop models for photon trajectories which, while possibly not representing underlying physical processes in precise detail, nevertheless are useful when determining dosimetry or analyzing spectroscopic data. Physical descriptions of light propagation in optically turbid media already have been developed at a number of levels of complexity. The classical approach, originally directed towards applications in astronomy, is based on transport theory but many useful features of photon distributions are equally well understood in terms of simpler phenomenological models [11,12]. Examples include diffusion [12,13] and random-walk models [14]. Simulation methods also have been applied extensively to this class of problems [15,16].

One advantage of the random-walk models has been their ability to produce relatively simple mathematical expressions for various quantities of interest. Our own applications of random-walk models mostly involve calculations of photon reemissions at an illuminated surface of thick tissue [14,17–19]. Of these, one important class of problems for remote sensing concerns intensity profiles of surface reemitted photons, measured as a function of the distance from the point of incidence of a continuous source. A second group relates to the case where light is injected as a pulse and information is obtained from the time distribution of the reemitted photons [9,10] or, in the frequency domain, the phase shift of a diffusive wave [20–22].

In our previous investigations the tissue was modeled as an infinitely thick homogeneous bulk medium. The present paper concerns reflection from, and transmission through, a slab of finite thickness. We begin, in Sec. II, by analyzing a random walk on an isotropic scattering lattice bounded by two absorbing planes. Expressions for path-length distributions, diffuse emission intensity profiles, and mean transit times are derived for both reflected and transmitted photons. Exact formulas for the path-length distributions are obtained which can be applied even when the thickness of the slab is only a few times the optical mean free path. We also derive variants of those expressions that are analytically somewhat more tractable. The latter are good approximations to the exact solutions when the slab is thick.

In Sec. III we present simulated Monte Carlo data relating to several of the derived analytical expressions. Particular attention is given to path-length distributions for relatively thin slabs, for which short-path photons can be of great importance. One motivation for this work has been to discern the circumstances under which formulas based on diffusion theory might fail to adequately represent the random walks of the photons [23]; hence, in addition to comparing simulated data with curves calculated by our random-walk theory, similar comparison is made with curves obtained from commonly used expressions derived from diffusion theory [13].

Results are discussed in Sec. IV. We also include a brief discussion of the effect of redefining lattice parameters in terms of transport-corrected scattering and absorption coefficients in order to account for scattering-angle anisotropy. An Appendix contains a compilation of random-walk-model expressions which have been rewritten in terms of real space-time variables.

II. THEORY

Our model essentially involves describing photon migration in an optically turbid medium by a discrete-time random walk on an isotropic scattering lattice. The separation between two neighboring lattice points represents the physical distance that a photon travels, on average, before its direction is randomized. We derive the joint probabilities that a photon emerges at a distance ρ on a

surface after n lattice steps, where ρ measures the axial distance from the point of insertion to the point of reemission. The latter is expressed in terms of a lattice unit given, for an exponential scattering-length distribution, as the root-mean-square of scattering length $\sqrt{2}\Sigma_s^{-1}$, where Σ_s is an appropriate "transport-corrected" scattering coefficient [19,24]. For a finite slab, which is the focus of this paper, one can derive the joint probabilities in reflection and transmission after taking appropriate boundary and initial conditions into account.

The surfaces of the slab are represented by two infinite planes at $z=0$ and $z=L$, where L is the thickness defined in units of lattice spacing. In both cases (reflection and transmission) one has to calculate the probability $Q_n(r)$ that the photon is at $\mathbf{r}=(x,y,z)$ at step n [14]. The two surfaces, $z=0$ and $z=L$ are absorbing, so $Q_n(r)$ is subject to the boundary conditions

$$Q_n(x,y,0)=Q_n(x,y,L)=0 \ . \tag{1}$$

The initial condition is specified as

$$Q_n(\mathbf{r})=\delta_{x,0}\delta_{y,0}\delta_{z,1} \ , \tag{2}$$

where δ_{ij} is a Kronecker delta, which means that photons are inserted normal to the surface and that randomization of direction occurs only after the first step. The $Q_n(r)$ can be expressed in terms of the Green's function for random walks taking place on a fully infinite lattice, i.e., $P_n(x,y,z|x',y',z')$, which is the probability that a photon initially at (x',y',z') is at (x,y,z) at step n. $P_n(\mathbf{r})$ is known from the theory of lattice random walks [25] to be given as

$$P_n(\mathbf{r})=\frac{1}{(2\pi)^3}\int_{-\pi}^{\pi}\int_{-\pi}^{\pi}\int_{-\pi}^{\pi} e^{-i(\mathbf{r}\cdot\theta)}\lambda^n(\theta)d\theta_1 d\theta_2 d\theta_3 \ , \tag{3}$$

where $\lambda(\theta)=\lambda(\theta_1,\theta_2,\theta_3)$ is the structure factor of the random walk (the "characteristic function"), defined in terms of the single-step displacement probabilities $\{p(\mathbf{j})\}$ as

$$\lambda(\theta)=\sum_{\{j\}} p(\mathbf{j})e^{-i(\mathbf{j}\cdot\theta)} \ . \tag{4}$$

For an isotropic random walk on a Cartesian lattice, $p(j)=\frac{1}{6}$ in all directions, and $\lambda(\theta)$ is given as

$$\lambda(\theta)=\tfrac{1}{3}(\cos\theta_1+\cos\theta_2+\cos\theta_3) \ . \tag{5}$$

Two probability distributions are of primary interest for a finite slab. The first is the probability that a random walker is absorbed at a point $(x,y,0)$ on the $z=0$ surface, given that it has not previously reached the plane $z=L$; the second is the probability that a random walker is absorbed at a point (x,y,L) on the $z=L$ surface, given that it has not previously returned to the plane $z=0$. Since $z=0$ and $z=L$ are perfectly absorbing boundaries, one can use the method of images [26] to show that Q_n can be expressed as

$$Q_n(\rho)=\sum_{k=-\infty}^{\infty}\{P_{n-1}(\rho,z-1+2kL) - P_{n-1}(\rho,z+1+2kL)\}e^{-\mu n} \ . \tag{6}$$

Optical absorption is taken into account through the term $e^{-\mu n}$, where μ is defined as the absorption coefficient per step. (The underlying assumption is that Beer's law applies to photon absorption in the medium.)

The joint probabilities, $\Gamma_R(n,\rho)$ and $\Gamma_T(n,\rho)$, which are, respectively, the probabilities that a photon emerges at the distance $\rho=(x^2+y^2)^{1/2}$ on the surface $z=0$ and $z=L$ after n steps (reflection and transmission), can be derived by setting

$$\Gamma_R(n,\rho)=\tfrac{1}{6}Q_{n-1}(x,y,1)e^{-\mu} \tag{7}$$

and

$$\Gamma_T(n,\rho)=\tfrac{1}{6}Q_{n-1}(x,y,L-1)e^{-\mu} \ . \tag{8}$$

When one replaces $Q_{n-1}(x,y,L-1)$, for example, by the expressions given in Eqs. (3) and (6), the joint probability in the transmission mode, $\Gamma_T(n,\rho)$, can be derived as

$$\Gamma_T(n,\rho)=\frac{e^{-\mu n}}{6(2\pi)^3}\sum_{k=-\infty}^{\infty}\int_{-\pi}^{\pi}\int_{-\pi}^{\pi}\int_{-\pi}^{\pi} e^{-i(x\theta_1+y\theta_2)}\{e^{-i[(2k+1)L-2]\theta_3}-e^{-i[(2k+1)L]\theta_3}\} \times[\tfrac{1}{3}(\cos\theta_1+\cos\theta_2+\cos\theta_3)]^{n-2}d\theta_1 d\theta_2 d\theta_3 \ . \tag{9}$$

Before we reduce Eq. (9) to a different form, let us first examine an analogous expression for the unconditioned probability distribution, $\Gamma_T(n)$. The latter is the distribution of step lengths for those photons that are transmitted through the slab regardless of where they exit along the surface. This quantity is derived from Eq. (9) according to

$$\Gamma_T(n)=\sum_{x=-\infty}^{\infty}\sum_{y=-\infty}^{\infty}\Gamma_T(n,\rho) =\frac{e^{-\mu n}}{6(2\pi)^3}\sum_{k=-\infty}^{\infty}\int_{-\pi}^{\pi}\int_{-\pi}^{\pi}\int_{-\pi}^{\pi}\sum_{m=-\infty}^{\infty}\delta\left[\frac{\theta_1}{2\pi}-m\right]\sum_{m'=-\infty}^{\infty}\delta\left[\frac{\theta_2}{2\pi}-m'\right] \times\{e^{-i[(2k+1)L-2]\theta_3}-e^{-i[(2k+1)L]\theta_3}\}[\tfrac{1}{3}(\cos\theta_1+\cos\theta_2+\cos\theta_3)]^{n-2}d\theta_1 d\theta_2 d\theta_3 \tag{10a}$$

when, in order to obtain Eq. (10a), we observed that the sums over x and y can be expressed as $\sum_{m=-\infty}^{\infty}e^{i(m\theta)}=\sum_{m=-\infty}^{\infty}\delta(\theta_1/2\pi-m)$, where $\delta(\ )$ is the Dirac delta function. Because only the $m=0$ and $m'=0$ terms contribute to the integral given in Eq. (10a), $\Gamma_T(n)$ can be rewritten as

$$\Gamma_T(n)=\frac{e^{-\mu n}}{12\pi}\int_{-\pi}^{\pi}\sum_{k=-\infty}^{\infty}\{e^{-i[(2k+1)L-2]\theta}-e^{-i[(2k+1)L]\theta}\}[\tfrac{1}{3}(2+\cos\theta)]^{n-2}d\theta\ . \tag{10b}$$

Thus, if we again use the identity $\sum_{k=-\infty}^{\infty}e^{i(2Lk\theta)}=\sum_{m=-\infty}^{\infty}\delta(\theta L/\pi-m)$ and then perform the coordinate transformation $\theta L/\pi=v$, we find that $\Gamma_T(n)$ can be expressed as

$$\Gamma_T(n)=\frac{e^{-\mu n}}{12\pi}\int_{-L}^{L}e^{-iv\pi}(e^{2iv\pi/L}-1)\sum_{m=-\infty}^{\infty}\delta(v-m)\{\tfrac{1}{3}[2+\cos(\pi v/L)]\}^{n-2}dv\ . \tag{10c}$$

Finally, after performing the integration and after rearranging terms, we obtain the following expression for the step-length distribution $\Gamma_T(n)$:

$$\Gamma_T(n)=\frac{e^{-\mu n}}{6L}\sum_{m=1}^{L}(-1)^{m+1}[1-\cos(2\pi m/L)]\{\tfrac{1}{3}[2+\cos(\pi m/L)]\}^{n-2}\ . \tag{11a}$$

Because on this lattice all steps are of equal length, $\Gamma_T(n)$ in this case is equivalent to the path-length distribution of transmitted photons. Note that a useful correlate to Eq. (11a) can be obtained, for large values of n, by making the Gaussian approximation $(\frac{1}{3}[2+\cos(\pi m/L)])^n\approx\exp(-nm^2\pi^2/6L^2)$, in which case Eq. (11a) becomes

$$\Gamma_T(n)\approx\frac{e^{-\mu n}}{6L}\sum_{m=1}^{L}(-1)^{m+1}[1-\cos(2\pi m/L)]e^{-(n-2)m^2\pi^2/6L^2}\ . \tag{11b}$$

An equivalent formula, derived by using the Gaussian approximation earlier in the derivation, is

$$\Gamma_T\approx\left[\frac{1}{24\pi(n-2)}\right]^{1/2}\sum_{k=-\infty}^{\infty}\{e^{-[3/2(n-2)][2k+1)L-2]^2}-e^{-[3/2(n-2)][(2k+1)L]^2}\}e^{-\mu n}\ . \tag{11c}$$

We now observe that the expression for $\Gamma_T(n,\rho)$, given by Eq. (9), can be reduced by similar procedures. One finds, in analogy with Eq. (11a),

$$\Gamma_T(n,\rho)=\frac{e^{-\mu n}}{6L(2\pi)^3}\int_{-\pi}^{\pi}\int_{-\pi}^{\pi}\sum_{k=-\infty}^{\infty}\sum_{m=1}^{L}[1-\cos(2\pi m/L)]\{e^{-i[(2k+1)L-2]\theta_3}-e^{-i[(2k+1)L]\theta_3}\}$$
$$\times\{\tfrac{1}{3}[\cos\theta_1+\cos\theta_2+\cos(\pi m/L)]\}^{n-2}d\theta_1 d\theta_2\ . \tag{12a}$$

The integrals in this expression are easily performed if we first make the approximation, valid for large n, that $(\frac{1}{3}[\cos\theta_1+\cos\theta_2+\cos(m\pi/L)])^{n-2}\approx\exp(-[(n-2)/6][\theta_1^2+\theta_2^2+m^2\pi^2/L^2])$. In this case Eq. (12a) takes the form

$$\Gamma_T(n,\rho)\approx\frac{e^{-\mu n}}{4\pi L}\sum_{m=1}^{L}(-1)^{m+1}\{[1-\cos(2\pi m/L)]\}e^{-(n-2)m^3\pi^2/6L^2}\frac{1}{(n-2)}e^{-3\rho^2/2(n-2)}\ . \tag{12b}$$

As expected, the result given in Eq. (11b) is found by integrating $\Gamma_T(n,\rho)$, as given by Eq. (12b), over $2\pi\rho\,d\rho$.

The expression given in Eq. (12b) may be written alternatively as [cf. Eq. (11c)]

$$\Gamma_T(n,\rho)=\frac{\sqrt{3}}{2}\left[\frac{1}{2\pi(n-2)}\right]^{3/2}e^{-3\rho^2/2(n-2)}\sum_{k=-\infty}^{\infty}\left[\exp\left[-\frac{3}{2}\frac{[(2k+1)L-2]^2}{n-2}\right]-\exp\left[-\frac{3}{2}\frac{[(2k+1)L]^2}{n-2}\right]\right]e^{-\mu n}. \tag{12c}$$

An expression for $\Gamma_T(\rho)$, which is proportional to the total amount of energy emitted in a ring defined by the radii ρ and $\rho+d\rho$, can be obtained by integrating Eq. (12c) over n. We find

$$\Gamma_T(\rho)=\frac{e^{-2\mu}}{4\pi}\sum_{k=-\infty}^{\infty}\left[\frac{e^{-(6\mu\{\rho^2+[(2k+1)L-2]^2\})^{1/2}}}{\sqrt{\rho^2+[(2k+1)L-2]^2}}-\frac{e^{-(6\mu\{\rho^2+[(2k+1)L]^2\})^{1/2}}}{\sqrt{\rho^2+[(2k+1)L]^2}}\right]\ . \tag{13}$$

Then, the *total* amount of energy absorbed at $z=L$ can be obtained by integrating Eq. (13) over ρ, which yields the following expression for the transmittance $T_0(\mu)$ of a finite slab,

$$T_0(\mu)=\frac{e^{-2\mu}}{\sqrt{24\mu}}\sum_{k=-\infty}^{\infty}\{e^{-\sqrt{6\mu}[|(2k+1)L-2|]}-e^{-\sqrt{6\mu}[|2k+1)L|]}\}$$
$$=\frac{e^{-2\mu}}{\sqrt{24\mu}}\left[\frac{\cosh(\sqrt{24\mu})-1}{\sinh(\sqrt{6\mu}L)}\right]\ . \tag{14}$$

Another quantity of interest is the expected number of steps taken by a photon before it is reemitted at surface $z=L$.

This expression can be derived according to

$$\langle n|\rho\rangle_T=\frac{\sum_{n=2}^{\infty} n\Gamma_T(n,\rho)}{\sum_{n=2}^{\infty}\Gamma_T(n,\rho)}\ , \tag{15}$$

where in the continuum limit the summations can be replaced by integrations over n. One thus finds from Eq. (12c)

$$\langle n|\rho\rangle_T=\frac{\int_0^{\infty}(n+2)\Gamma_T((n+2),\rho)dn}{\int_0^{\infty}\Gamma_T((n+2),\rho)dn}$$

$$=2+\left[\frac{3}{2\mu}\right]^{1/2}\frac{\sum_{k=-\infty}^{\infty}[\exp(-\alpha\sqrt{6\mu})-\exp(-\beta\sqrt{6\mu})]}{\sum_{k=-\infty}^{\infty}\left[\frac{\exp(-\alpha\sqrt{6\mu})}{\alpha}-\frac{\exp(-\beta\sqrt{6\mu})}{\beta}\right]}\ , \tag{16}$$

where $\alpha=\sqrt{\rho^2+[(2k+1)L-2]^2}$ and $\beta=\sqrt{\rho^2+[(2k+1)L]^2}$.

Analogous expressions can be obtained for photons which are emitted at the upper surface, at $z=0$. We find, corresponding to Eqs. (11a), (12c), (13), (14), and (16), the following expressions for reflected photons: (i) For the path-length distribution,

$$\Gamma_R(n)=\frac{e^{-\mu n}}{6L}\sum_{m=1}^{L}[1-\cos(2\pi m/L)]\{\tfrac{1}{3}[2+\cos(\pi m/L)]\}^{n-2} \tag{17a}$$

$$\approx\frac{1}{\sqrt{12}}\left[\frac{1}{2\pi(n-2)}\right]^{1/2}\sum_{k=-\infty}^{\infty}\left[\exp\left[-\frac{3}{2(n-2)}[2kL]^2\right]-\exp\left[-\frac{3}{2(n-2)}[(2k+2)L]^2\right]\right]e^{-\mu n}\ ; \tag{17b}$$

(ii) for the joint distribution,

$$\Gamma_R(n,\rho)=\frac{\sqrt{3}}{2}\left[\frac{1}{2\pi(n-2)}\right]^{3/2}e^{-3\rho^2/2(n-2)}\sum_{k=-\infty}^{\infty}\left[\exp\left[-\frac{3}{2}\frac{[2kL]^2}{n-2}\right]-\exp\left[-\frac{3}{2}\frac{[(2k+2)L]^2}{n-2}\right]\right]e^{-\mu n}\ ; \tag{18}$$

(iii) for the intensity distribution

$$\Gamma_R(\rho)=\frac{e^{-2\mu}}{4\pi}\sum_{k=-\infty}^{\infty}\left[\frac{e^{-\sqrt{6\mu(\rho^2+[2kL]^2)}}}{\sqrt{\rho^2+[2kL]^2}}-\frac{e^{-\sqrt{6\mu[\rho^2+[(2k+2)L]^2}}}{\sqrt{\rho^2+[(2k+2)L]^2}}\right]\ ; \tag{19}$$

(iv) for the reflectance,

$$R_0(\mu)=\frac{e^{-2\mu}}{\sqrt{24\mu}}\left[1-\exp(-\sqrt{24\mu})+\frac{2[1-\cosh(\sqrt{24\mu})]}{\exp(\sqrt{24\mu}L)-1}\right]\ ; \tag{20}$$

and (v) for the expected step length,

$$\langle n|\rho\rangle_R=2+\left[\frac{3}{2\mu}\right]^{1/2}\frac{\sum_{k=-\infty}^{\infty}[\exp(-\alpha'\sqrt{6\mu})-\exp(-\beta'\sqrt{6\mu})]}{\sum_{k=-\infty}^{\infty}\left[\frac{\exp(-\alpha'\sqrt{6\mu})}{\alpha'}-\frac{\exp(-\beta'\sqrt{6\mu})}{\beta'}\right]}\ , \tag{21}$$

where $\alpha'=\sqrt{\rho^2+[2kL]^2}$ and $\beta'=\sqrt{\rho^2+[2kL+2]^2}$.

Equations (11), (12c), (13), (14), (16), and (17) comprise a complete set of formulas for analyzing actual measurements if the parameters used in random-walk theory, ρ, n, μ, can be related to real time and space variables (t,r) and to parameters usually used in optics such as the absorption and scattering cross sections (Σ_a and Σ_s). For isotropic scattering, and when the scattering lengths are exponentially distributed, appropriate transformations are [19,24]

$$\rho=r\frac{\Sigma_s}{\sqrt{2}}\ ,\quad \mu=\frac{\Sigma_a}{\Sigma_s}\ ,\quad n=\Sigma_s ct=\Sigma_s l\ , \tag{22}$$

where c is the speed of light in tissue and l is the path length in real space, related to the time as $l=ct$. (In general, the distance variables on the lattice, such as ρ, can

be expressed as real distances divided by the root-mean-square scattering length [14].)

Because these expressions were derived for a discrete lattice model, they need to be modified slightly in order that they be valid for photon migration in a continuum space. In a continuum space photons cross the boundaries when they escape, whereas they are absorbed exactly at $z=L$ in a random-walk model on a discrete lattice. To account for this difference one may place the lower boundary of the slab at $z=L+\epsilon$ (where ϵ is small), rather than at $z=L$. But, on a discrete lattice, the probability of reaching $L+\epsilon$ is equal to the probability of being at $L+1$. Hence, as shall be shown in the next section, to properly account for photon migration near the boundaries, we find that the value of L appearing on the preceding analytical expressions must be increased by 1; also, except for factors which account for absorption, the step number n, too, should be increased by 1. For example, the expression for $\Gamma_T(n)$ given by Eq. (11a) becomes, for a continuum,

$$\Gamma_T(l)=\frac{e^{-\Sigma_a l}}{6(L+1)}\sum_{m=1}^{L+1}(-1)^{m+1}(1-\cos[2\pi m/(L+1)])\times(\tfrac{1}{3}\{2+\cos[\pi m/(L+1)]\})^{l-1}\ . \tag{23}$$

Real-variable expressions for several of the above distributions are presented, below, in the Appendix.

III. SIMULATIONS

Different sets of Monte Carlo calculations were performed in order to substantiate analytical results obtained in the previous section. These calculations were done for several slab thicknesses and different values of anisotropy coefficient ($g=0$, 0.9). The number of simulations for any particular conditions was of the order of 10^6–10^8, which yielded statistically meaningful results even for time-resolved distributions. Scattering lengths here were exponentially distributed, with the mean scattering length taken to be 1. The scattering angle was determined from the cumulative probability distribution of the Henyey-Greenstein phase function [27]. Details of the Monte Carlo procedures used for these simulations are described elsewhere [19,24].

Figure 1 shows the results of Monte Carlo simulations of the distribution of total path lengths experienced by photons which traverse the slab. The open circles represent the results of simulations, and the solid lines have been calculated from the expression for $\Gamma_T(l)$ given in Eq. (23). All results shown in this figure were obtained for $\mu=0$, i.e., in the absence of absorption. Figure 1(a) shows results of simulations for a continuum, for $\mathcal{L}=10\sqrt{2}$ where $\mathcal{L}$ is the thickness of the slab measured in units of mean scattering length Σ_s^{-1}. The corresponding analytical expression for $\Gamma_T(l)$ has been determined for the scaled thickness $L=10$, related to the real distance according to Eq. (22), viz.,

$$\mathcal{L}=\sqrt{2}L\ . \tag{24}$$

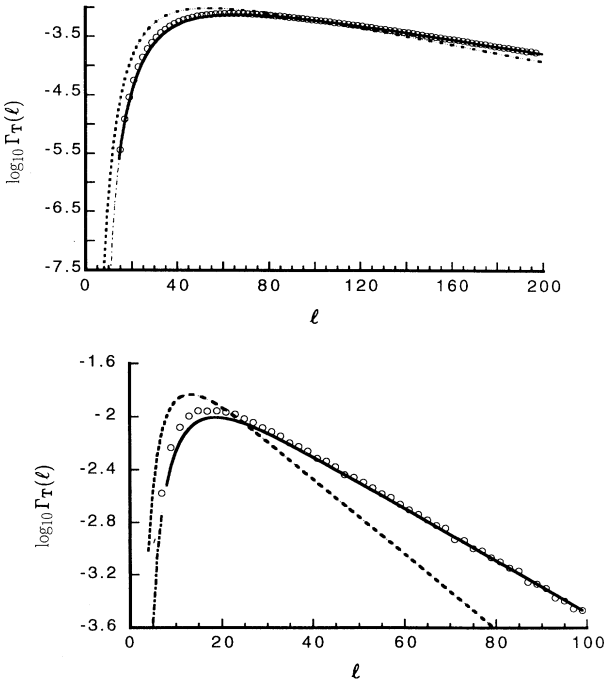

FIG. 1. Logarithm of the path-length distribution, $\Gamma_T(l)$, calculated by Monte Carlo simulations and random-walk and diffusion theories. (a) Slab thickness $\mathcal{L}=10\sqrt{2}$. (b) Slab thickness $\mathcal{L}=5\sqrt{2}$. Here, the absorption per unit scattering length, μ, has been set to zero. The solid lines represent values that have been obtained from Eq. (23), based on random-walk theory. The dashed lines have been calculated from an expression derived from diffusion theory [13]—see Eq. (25).

The evaluation of Eq. (23) is shown here by a solid line for values of $l\geq\mathcal{L}$, as no photons can cross the slab unless their total path length exceeds this minimal value; the values of Eq. (23) for lower values of l are shown by the thin dashed line. For comparison we indicate by the dotted line, for $\mathcal{L}=10\sqrt{2}$, some results of calculations based on an analytic expression derived from the optical diffusion equation [13],

$$\Gamma_T(l)\sim\frac{e^{-\mu l}}{l^{3/2}}[(\mathcal{L}-1)e^{-3(\mathcal{L}-1)^2/4l}-(\mathcal{L}+1)e^{-3(\mathcal{L}+1)^2/4l}+(3\mathcal{L}-1)e^{-3(3\mathcal{L}-1)^2/4l}-(3\mathcal{L}+1)e^{-3(3\mathcal{L}+1)^2/4l}]\ . \tag{25}$$

We find that the Monte Carlo results are represented very well by our analytic random-walk theory. However, whereas the diffusion theory expression given by Eq. (25) here provides a fair approximation for large values of path length, it fails to adequately represent $\Gamma_T(l)$ for smaller values of l. Similar correspondences are observed in Fig. 1(b), where $\Gamma_T(l)$ is given for a significantly thinner slab, $\mathcal{L}=5\sqrt{2}$. Note that the agreement between the Monte Carlo data and points derived by simple evaluation of Eq. (25) is much poorer, even at high values of l (see the discussion).

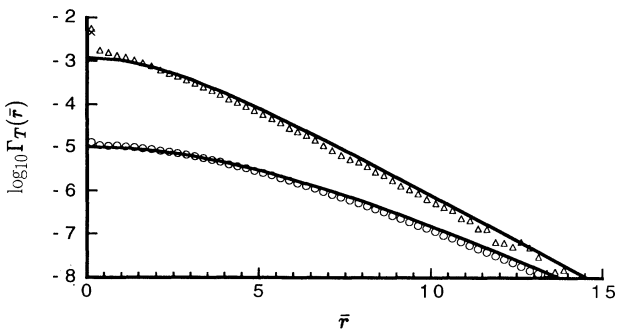

FIG. 2. Results obtained from Monte Carlo simulations of intensity profiles, $\Gamma_T(\bar{r})$, for two thicknesses $\mathcal{L}=10\sqrt{2}$ (○) and $\mathcal{L}=5\sqrt{2}$ (△). The solid lines are calculated according to random-walk theory ($\mu=0.1$). The cross (×) represents the purely ballistic photons (for $\mathcal{L}=5\sqrt{2}$), which are not taken into account in the random-walk analysis.

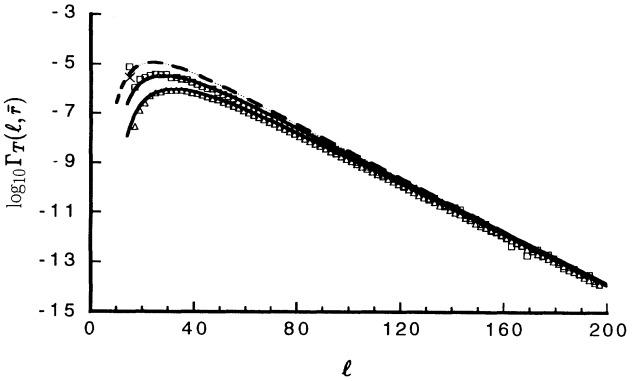

FIG. 3. The distribution of path lengths, $\Gamma_T(l,\bar{r})$, for two points $\bar{r}=0.175$ (□) and $\bar{r}=6.89$ (△), obtained from Monte Carlo simulations ($\mathcal{L}=10\sqrt{2}, \mu=0.1$). The solid lines were obtained from random-walk theory according to Eq. (A2); the dashed line has been obtained from an expression derived from optical diffusion theory [Eq. (25)]. The cross (×) represents the ballistic photons which are transmitted when $\bar{r}=0.175$.

In Fig. 2 we show intensity profiles $\Gamma_T(\bar{r})$, where $\bar{r}\equiv\Sigma_s r$ is the real distance expressed in terms of the mean scattering length. The values of slab thickness are the same as in Fig. 1 ($\mathcal{L}=5\sqrt{2}$, $10\sqrt{2}$). Here, the value of the absorbance per mean scattering length is taken as $\mu=0.1$. The circles are the results of the simulations, and the solid lines are calculated according to Eq. (A1) [cf. Eq. (13)]. Again, the correspondence between simulation and theory is quite good, except for very small values of r where the Monte Carlo results show the presence of ballistic photons which leave the slab without experiencing any scattering. The cross (×) is the value obtained by including ballistic photons, calculated according to the expression $\Gamma_T(l)_{\text{ballistic}}=\exp[-(1+\mu)\mathcal{L}]$, which accounts for the nonzero absorption assumed for this example.

A quantity of particular interest [9,10] is the distribution of path lengths of those photons which leave at a particular point $\bar{r}$, $\Gamma_T(l,\bar{r})$. Figure 3 shows the results of Monte Carlo simulations for $\mathcal{L}=10\sqrt{2}$ and $\mu=0.1$, for two values of $\bar{r}$ ($\bar{r}=0.175$ and $\bar{r}=6.89$). The solid lines were obtained from Eq. (A2) [cf. Eq. (12c)]; the dashed line, calculated for $\bar{r}=0.175$, has been obtained from an expression derived from optical diffusion theory [13],

$$\Gamma_T(l,r)\sim\frac{e^{-\mu l}e^{-3\Sigma_s r^2/4l}}{l^{5/2}}[(\mathcal{L}-1)e^{-3(\mathcal{L}-1)^2/4l}-(\mathcal{L}+1)e^{-3(\mathcal{L}+1)^2/4l}+(3\mathcal{L}-1)e^{-3(3\mathcal{L}-1)^2/4l}-(3\mathcal{L}+1)e^{-3(3\mathcal{L}+1)^2/4l}]\ . \tag{26}$$

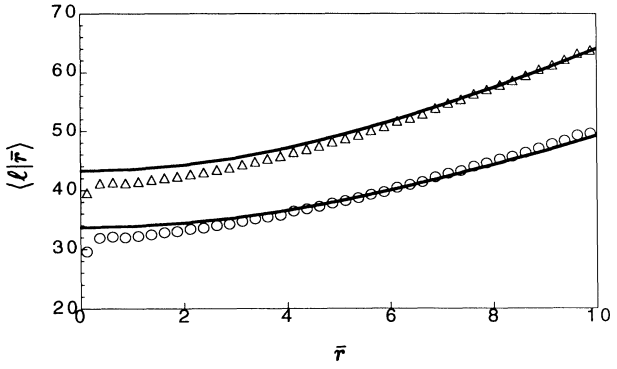

FIG. 4. Mean path length $\langle l|\bar{r}\rangle$. Results of Monte Carlo simulations for $\mu=0.05$ (△) and $\mu=0.1$ (○) are compared with the theoretical expression given by Eq. (A3). ($\mathcal{L}=10\sqrt{2}$.)

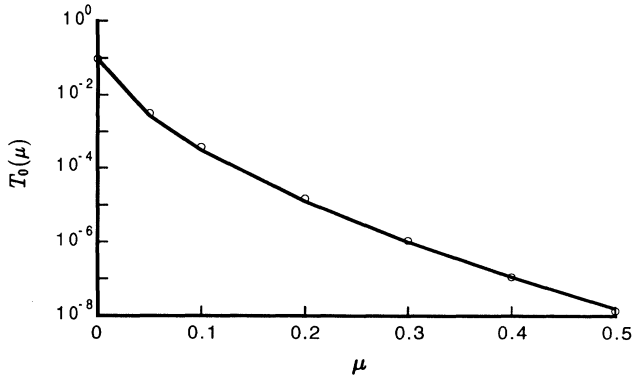

FIG. 5. Total transmission, $T_0(\mu)$. Circles are the results of Monte Carlo simulations; the solid line is obtained according to the random-walk theory expression given by Eq. (A4). Slab thickness: $\mathcal{L}=10\sqrt{2}$.

Whereas the values obtained from the random-walk expressions fit the data quite well, the diffusion-theory results again show poorer agreement at smaller values of l. Here, as in Fig. 2, the cross ($\times$) represents ballistic photons.

A related quantity, the mean path length, $\langle l|\bar{r}\rangle$, is shown in Fig. 4, for $\mathcal{L}=10\sqrt{2}$, for two values $\mu=0.05$ and $\mu=0.10$. The solid lines have been calculated from the random-walk theory expression given by Eq. (A3). Finally, in Fig. 5, results of simulations of the total transmission $T_0(\mu)$ (also for $L=10\sqrt{2}$) are compared with values calculated from Eq. (A4) (solid line). In both cases, agreement between simulations and theory again is quite satisfactory.

IV. SUMMARY AND DISCUSSION

This work attempts to provide mathematical expressions for quantities relating to the propagation of light within a slab of an optically turbid, multiply scattering medium. Using a discrete lattice model to describe photon transport, we derived expressions for several measurable quantities. These include the intensity profiles along the external surfaces of the medium, the distribution of path lengths of emergent photons, and reflection and transmission coefficients. Although our derivations involved dimensionless parameters such as ρ, n, and μ, appropriate substitutions, such as those presented in Eq. (22), lead to equations with real time and space as variables. Examples of such quantities are presented in the Appendix.

To test our analysis we performed Monte Carlo simulations and compared results with the mathematical expressions. The good agreement between simulations and theory suggests that the random-walk approach is an appropriate way to investigate aspects of photon migration in highly turbid media. The expressions given in Eq. (11a) for the path-length distribution of transmitted photons is particularly appealing, since it includes a natural theoretical cutoff for photons whose path lengths are smaller than the slab thickness. This cutoff is mathematically exact for an assumed constant scattering-length distribution, although for an exponential distribution of scattering lengths (corresponding to randomly distributed scatterers) the natural cutoff occurs at $\mathcal{L}$ instead of L [see Eq. (24)].

Since we are dealing with an exponential distribution of scattering lengths, there always is a finite probability that a photon is transmitted through the slab without having been scattered. Such photons may be discerned for small ρ (Fig. 2) or small path length (Fig. 3). As previously indicated, this probability is equal to $\exp[-(1+\mu)\mathcal{L}]$ so, for thicker slabs, the probability of transmitting such ballistic photons is vanishingly small. No analytical theory for light migration can handle the effect of all nearly ballistic photons; for certain purposes, though, transport through slabs of small thickness can be treated by adding the exponential term associated with truly ballistic photons, given above, to the analytical transport expression given by Eq. (14) (see Figs. 3 and 4).

Strictly speaking, all of the equations given in the bulk of the paper hold only for processes involving isotropic scattering cross sections. However, we implicitly assumed that these isotropic models are generally applicable if one properly redefines lattice parameters in terms of transport-corrected parameters. Since scattering in tissues is strongly peaked in the forward direction, application of our theory requires the explicit introduction of transport-corrected scattering and absorption coefficients in order to take into account the effect of anisotropy. The latter commonly are characterized in terms of the expected value of the cosine of the scattering angle $g=\int_0^{\pi}\cos(\theta)P(\theta)\sin(\theta)\,d\theta$, where $P(\theta)$ is the scattering angle distribution. Previously, we showed that, although the scaling of these coefficients depends on the scattering-length distribution [24], for exponentially distributed scattering lengths the transport corrected cross sections are given as $\Sigma_s'=(1-g)\Sigma_s$, $\Sigma_a'=\Sigma_a$. This scaling also commonly is used in the diffusion approximation of transport theory [28].

Figure 6 shows the logarithm of path-length distribution, $\Gamma_T(l)$, calculated by Monte Carlo simulations for $g=0$ and $g=0.9$. These results confirm that the $(1-g)$ scaling of the scattering cross section is quite adequate for long-path photons, whereas for short-path photons this scaling fails. This observation is in accord with our similar finding for reflectance experiments, which suggested that another scaling relation has to be used for anisotropic scattering of short-path photons [19]. The scaling required for such photons (sometimes referred to as "snake" photons) becomes important when one deals with tomographic imaging systems which utilize only prompt photons. This problem will be discussed in future publications.

We have limited our study to the time domain, but there is a growing interest in using frequency-domain analysis in order to describe photon migration in turbid media [20–22]. This goal is easily realized by taking the Fourier transform of Eq. (12a) which can be done analytically. Furthermore, the expression for the mean path length, Eq. (16), can be directly related to the phase shift of a modulated diffusing wave [20].

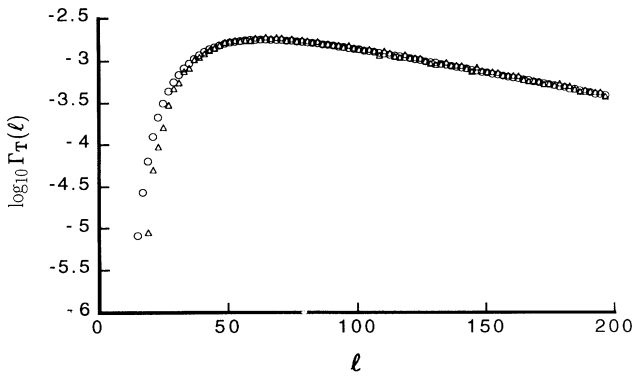

FIG. 6. Logarithm of the path-length distribution, $\Gamma_T(l)$, obtained from Monte Carlo simulations for two different values of anisotropy coefficient: $g=0$ (○); $g=0.9$ (△). Slab thickness: $\mathcal{L}=10\sqrt{2}$.

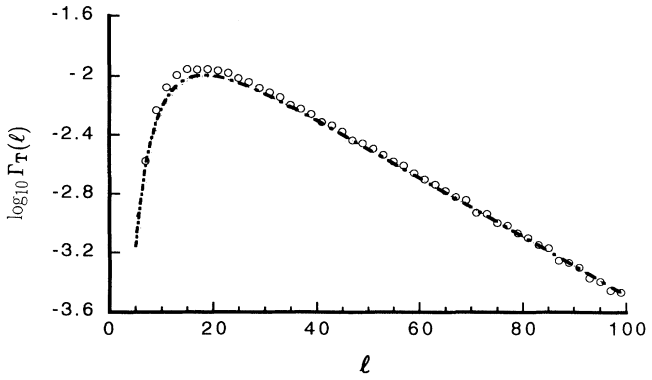

FIG. 7. Logarithm of the path-length distribution, $\Gamma_T(l)$. Data points are identical to those shown in Fig. 1(b). Dashed line pertains to the values obtained from a modified diffusion theory expression (see text).

Finally, as we did for random-walk theory, it is possible to modify results based on the diffusion approximation in order to better fit the long-time behavior for slabs of small thickness. The main idea is to replace the real thickness of the slab by $\mathcal{L}+\sqrt{2}$ and increase the time by $t_0=(\Sigma_s c)^{-1}$. Whereas similar adjustment of random-walk theory (RWT) has a theoretical basis, this kind of modification of the diffusion approximation is somewhat arbitrary. Nonetheless, as shown in Fig. 7 where we compare the simulated data first given in Fig. 1(b) with the modified diffusion theory results, we see that the long-time behaviors now agree quite well. With this modification, the discrepancy between theory and simulation is mitigated, also, for short-path photons.

APPENDIX: REAL VARIABLE EXPRESSIONS FOR RWT RESULTS

The following are quantities derived by random-walk theory on a lattice, but here expressed in terms of real variables r and l (distance and path length) and bulk optical cross sections Σ_a and Σ_s. Note that in calculating the curves shown in the text, Σ_s always was set equal to unity. In order to make explicit connection to the text above, one should make the substitution $\bar{r}=\Sigma_s r$ in the following expressions.

The diffuse intensity of transmitted photons, expressed as a function of real distance r from the optical axis, is given as [cf. Eq. (13)]

$$\Gamma_T(r)=\frac{e^{-2\Sigma_a/\Sigma_s}}{2\sqrt{2}\pi\Sigma_s^{-1}}\sum_{k=-\infty}^{\infty}\left[\frac{\exp(-3\Sigma_a\Sigma_s\{r^2+[(2k+1)d'-2\sqrt{2}\Sigma_s^{-1}]^2\})^{1/2}}{\{r^2+[(2k+1)d'-2\sqrt{2}\Sigma_s^{-1}]^2\}^{1/2}}-\frac{\exp(-3\Sigma_s\Sigma_s\{r^2+[(2k+1)d']^2\})^{1/2}}{\{r^2+[(2k+1)d']^2\}^{1/2}}\right]. \tag{A1}$$

In Eq. (A1), the symbol d' represents the corrected thickness of the slab, which is related to the actual thickness d by the expression $d'=d+\sqrt{2}\Sigma_s^{-1}$.

Similarly, the path-length distribution of transmitted photons which emerge from the scattering medium at point r is given as [cf. Eq. (12c)]

$$\Gamma_T(l,r)=\frac{\sqrt{3}\Sigma_s^2}{2}\left[\frac{1}{2\pi(\Sigma_s l-2)}\right]^{3/2}e^{-3\Sigma_s r^2/4(l-2\Sigma_s^{-1})}\times\sum_{k=-\infty}^{\infty}\left[\exp\left[-\frac{3}{4}\frac{[(2k+1)d'-2\sqrt{2}\Sigma_s^{-1}]^2}{l-2\Sigma_s^{-1}}\right]-\exp\left[-\frac{3}{4}\frac{[(2k+1)d']^2}{l-2\Sigma_s^{-1}}\right]\right]e^{-\Sigma_a l}, \tag{A2}$$

and the expected value of the path length may be expressed as [cf. Eq. (16)]

$$\langle n|\rho\rangle_T=2\Sigma_s^{-1}+\left[\frac{3\Sigma_s}{4\Sigma_a}\right]^{1/2}\frac{\sum_{k=-\infty}^{\infty}\{\exp[-A(r)\sqrt{3\Sigma_a\Sigma_s}]-\exp[-B(r)\sqrt{3\Sigma_a\Sigma_s}]\}}{\sum_{k=-\infty}^{\infty}\left[\frac{\exp[-A(r)\sqrt{3\Sigma_a\Sigma_s}]}{A(r)}-\frac{\exp[-B(r)\sqrt{3\Sigma_a\Sigma_s}]}{B(r)}\right]}, \tag{A3}$$

where $A(r)=(r^2+[(2k+1)d'-2\sqrt{2}\Sigma_s^{-1}]^2)^{1/2}$ and $B(r)=\{r^2+[(2k+1)d']^2\}^{1/2}$.

Finally, the expression for the transmission takes the form [cf. Eq. (14)]

$$T_0(\Sigma_a,\Sigma_s)=\frac{e^{-2\Sigma_a/\Sigma_s}}{\sqrt{24\Sigma_a/\Sigma_s}}\left[\frac{\cosh(\sqrt{24\Sigma_a/\Sigma_s})-1}{\sinh(\sqrt{3\Sigma_a\Sigma_s}d')}\right]. \tag{A4}$$

[1] *Lasers in General Surgery,* edited by S. N. Joffe (Williams and Wilkins, Baltimore, 1989).
[2] R. Brancato and R. Pratesi, Lasers Light Ophthalmol. **1**, 119 (1987).
[3] T. J. Dougherty, CRC Crit. Rev. Oncol. Hematol. **2**, 83 (1984).
[4] W. M. Star, H. P. A. Marijnissen, H. Jansen, M. Zeijzer, and M. J. C. van Gemert, Photochem. Photobiol. **46**, 619 (1987).
[5] *Laser-Doppler Blood Flowmetry,* edited by A. P. Shepherd, Jr. and P. Å. Öberg (Kluwer Academic, Boston, 1990).
[6] K. K. Tremper and S. J. Barker, Anesthesiology **17**, 98 (1989).
[7] J. C. Hebden and R. A. Krueger, Med. Phys. **17**, 351 (1990).
[8] S. R. Arridge, P. van der Zee, D. T. Delpy, and M. Cope, Proc. Soc. Photo-Opt. Instrum. Eng. **1431**, 204 (1991).
[9] D. T. Delpy, M. Cope, P. van der Zee, S. Arridge, S. Wray, and J. Wyatt, Phys. Med. Biol. **33**, 1433 (1988).
[10] B. Chance, J. S. Leigh, H. Miyake, D. S. Smith, S. Nioka, R. Greenfeld, M. Finander, K. Kaufmann, W. Levy, M. Yound, P. Cohen, H. Yoshioka, and R. Boretsky, Proc. Natl. Acad. Sci. USA **85**, 4971 (1988).
[11] H. C. van de Hulst, *Multiple Light Scattering* (Academic, New York, 1980), Vols. 1 and 2.
[12] A. Ishimaru, *Wave Propagation and Scattering in Random Media* (Academic, New York, 1978), Vol. 1.
[13] M. Patterson, B. Chance, and B. C. Wilson, Appl. Opt. **28**, 2331 (1989).
[14] R. Bonner, R. Nossal, S. Havlin, and G. H. Weiss, J. Opt. Soc. Am. A **4**, 423 (1987)
[15] M. Keijzer, S. L. Jacques, S. A. Prahl, and A. J Welch, Lasers Surg. Med. **9**, 148 (1989).
[16] S. T. Flock, M. S. Patterson, B. C. Wilson, and D. R. Wyman, IEEE Trans. Biomed. Engr. **BME-36**, 1162 (1989).
[17] R. Nossal, R. F. Bonner, and G. H. Weiss, Appl. Opt. **28**, 2238 (1989).
[18] G. H. Weiss, R. Nossal, and R. F. Bonner, J. Mod. Opt. **36**, 349 (1989).
[19] A. H. Gandjbakhche, R. Nossal, and R. F. Bonner, Appl. Opt. **32**, 504 (1993).
[20] J. Fishkin, E. Gratton, M. J. van de Ven, and W. W. Mantulin, Proc. Soc. Photo-Opt. Instrum. Eng. **1431**, 122 (1991).
[21] E. M. Sevick, B. Chance, J. Leigh, S. Nioka, and M. Maris, Anal. Biochem. **195**, 330 (1991).
[22] A. Knüttel, J. M. Schmitt, and J. R. Knutson, Appl. Opt. **32**, 381 (1993).
[23] K. M. Yoo, F. Liu, and R. R. Alfano, Phys. Rev. Lett. **64**, 2647 (1990).
[24] A. H. Gandjbakhche, R. F. Bonner, and R. Nossal, J. Stat. Phys. **69**, 35 (1992).
[25] G. H. Weiss and R. J. Rubin, Adv. Chem. Phys. **52**, 363 (1983).
[26] P. M. Morse and H. Feshbach, *Methods of Theoretical Physics* (McGraw-Hill, New York, 1953).
[27] L. G. Henyey and J. L. Greenstein, Astrophys. J. **93**, 70 (1941).
[28] J. J. Duderstadt and L. J. Hamilton, *Nuclear Reactor Analysis* (Wiley, New York, 1976).